Supporting Figure legends

Figure 1 supplement 1: The αβ-tubulin binding capacities of TOG1-TOG2 monomers and dimers and the non-equivalent exchange of αβ-tubulin by TOG1 and TOG2.

A, D, G, J) Top shows models for Alp14 TOG array constructs used studied for tubulin binding respectively and in order: Yeast Alp4-monomer (1-510), Alp14-dimer (residues 1-690) and Alp14-dimer-TOG1M, Alp14-dimer-TOG2M (inactivated TOG1 or TOG2 dimers), Bottom, SEC elution profiles for these constructs in complex with αβ-tubulin at 80-100 and 200 mM KCl at two molar ratios of TOG array subunit:αβ-tubulin. Note the largest Alp14 complexes form at 80-100 mM KCl in 1:2 molar ratio for Alp14-monomer, and 2:4 molar ratio for Alp14-dimer constructs. Colors of the ratios to the top left of each SDS-PAGE panel match those in traces described below. Note the formation of a second peak for αβ-tubulin in the 200 mM KCl conditions.

B, E, H, K) SDS-PAGE of the four SEC traces shown in each panel above A,D,F,I respectively. Top left corner shows the molar ratio in the same color as the trace above. Note the dissociation of αβ-tubulin, which forms a second peak at 200 mM KCl. Note, Alp14-dimer TOG1M mutant fully dissociates at 200 mM, while Alp14-dimer-TOG2M remains mostly bound to αβ-tubulin at 200 mM KCl.

C, H, I, L) Schematic Models, similar to Figure 1F, for wt-Alp14-monomer, wt-Alp14-dimer, TOG2M, TOG1M in binding αβ-tubulins at 100 mM and 200

mM KCl revealing the non-equivalent behavior of TOG1 and TOG2 domains in exchanging αβ-tubulins in response to a moderate change in ionic strength.

Figure 1 supplement 2: **Measured Masses and the αβ-tubulin binding stoichiometry to various TOG arrays and DRP binds each αβ-tubulin in TOG array complexes.**

A, D) Top shows models for DRP (yellow) binding to Alp14 constructs: wt-Alp4-monomer (1-510) and wt-Alp14-dimer (residues 1-690). Bottom, SEC elution profiles for these constructs in complex with αβ-tubulin at 80-100 and 200 mM KCl at two molar ratios of TOG array subunit:αβ-tubulin. Colors of the ratios to the top left of each SDS-PAGE panel match those in traces described below. Note the formation of a second peak for αβ-tubulin in the 200 mM KCl conditions, which includes both αβ-tubulin and DRP.

B, E) SDS-PAGE of the four SEC traces shown in each panel above A,D respectively. Top left corner shows the molar ratio in the same color as the trace above. Note that DRP binds each Alp14 complex and its stoichiometry matches αβ-tubulin. Note the dissociation of αβ-tubulin, which forms a second peak at 200 mM KCl.

C, F) Schematic Models for Alp14-monomer and Alp14-dimer, in binding αβ-tubulins at 80-100 mM and 200 mM KCl revealing the non-equivalent behavior of TOG1 and TOG2 domains in releasing αβ-tubulins. DRP can

access each β-tubulin interface suggesting that TOG arrays maintain αβ-tubulins in a non-polymerized state upon binding.

G) SEC-MALS traces for Alp14-monomer binding αβ-tubulin reveals masses of components and resulting complexes at 80-100 mM KCl. These data are summarized in table S1. Alp14-monomer (TOG1-TOG2) binds two αβ-tubulins at 80-100 mM KCl, each of which can be loaded with DRP.

H) SEC-MALS traces for Alp14-dimer binding αβ-tubulin at 2:4 molar ratio at 100 mM KCl or 200 mM KCl, respectively. These data are summarized in table S1.

I) SEC-MALS traces for Alp14-dimer binding to αβ-tubulin at 2:2 molar ratio 100 mM KCl or 200 mM KCl, respectively. These data are summarized in table S1.

J) SEC-MALS traces for Alp14-dimer-TOG1M and Alp14-dimer-TOG2M binding to αβ-tubulin at 2:4 molar ratio in 100 mM KCl. These data are summarized in table S1.

Figure 1 supplement 3: **Isothermal titration calorimetry (ITC) reveals Alp14-TOG1 and TOG2 αβ-tubulin binding affinities. (A)** Left panel, scheme for recombinant TOG1 and TOG2 domains studied and SDS-PAGE of purified 10 and 1 μM TOG1 and TOG2 domains. Right panel, Summary of measured αβ-tubulin binding affinities at 100 and 200 mM KCl. **(B, D)** Isothermal titration calorimetry traces for TOG1 (blue) binding to αβ-tubulin showing enthalpy and entropy measured at 100 and 200 mM KCl.

(C, F) Isothermal titration calorimetry traces for TOG2 (cyan) binding to αβ-tubulin showing enthalpy and entropy measured at 100 and 200 mM KCl.

Figure 2 supplement 1: X-ray crystallography and Structure determination of 2:4:4 Alp14-monomer:αβ-tubulin:DRP complexes

A) Images of square crystals of 1:2:2 sk-Alp14-monomer:αβ-tubulin:DRP assemblies.

B) Molecular replacement search results for αβ-tubulin placement in the unit cell. Note the distinct solution that leads to initial positioning.

C) Molecular replacement search results for TOG domain in the unit cell.

D) Initial Density map of electron density for the TOG square assembly after the placement of TOG domains based on initial molecular replacement. Note the presence of only the essential features of both TOG domains.

E) Density map of the TOG square assembly after one cycle of density modification. Note the appearance of density of the linker and associating interfaces. Density maps reveal TOG1 based on its C-terminal extension and jutting C-terminal α-helix.

F) Top view of the crystallographic unit cell revealing the packing arrangement revealing two 2:4:4 sk-Alp14-monomer:αβ-tubulin:DRP wheel-shaped complexes in the unit cell, shown in multiple colors. Bottom, a 90° rotation of the view in **F**, revealing the unit cell packing showing two complexes in the unit cell.

G) 4.4-Å resolution 2Fo-Fc electron density contoured at 1 σ of the native 2:4:4 sk-Alp14-monomer:$\alpha\beta$-tubulin:DRP structure.

H) 3.6-Å resolution 2Fo-Fc electron density contoured at 1σ of 2:4:4 sk-Alp14-SL:$\alpha\beta$-tubulin:DRP structure. Both **G** and **H** show the organization of the assembly and the modeled subunits.

I) Detailed close-up views of the electron density map in **H**. Top, view of TOG1 (orange)-TOG2 (red) in interface 1. The linker sequence is depicted as red with green density (difference Fourier map). Bottom, detailed view of DRP (yellow) in proximity to the α-tubulin of a neighboring TOG-bound $\alpha\beta$-tubulin (blue). Note the lack of interactions between DRP and α-tubulin.

J) View of DRP proximity to the α-tubulin of the neighboring tubulin dimer. Note the distances of residues are beyond 3.5-Å in most cases showing no pattern of direct interactions

K) View of second DRP of a non-crystallographic symmetry mate in the same orientation as shown in I.

Figure 2 supplement 2: Sequence conservation in TOG square interfaces across each TOG1 and TOG2 domains.

A) Top scheme for Alp14- TOG1, TOG2 and linker sequence. Bottom, Structure of TOG square with two TOG1 (Blue) and two TOG2 (cyan) domains forming interfaces via inter-HEAT repeat elements with the TOG1-TOG2 linker (red) sequence.

B) Sequence alignment of TOG1-TOG2 across multiple species with the invariant residues shown in purple, highly conserved residues in blue,

weakly conserved residues in cyan, and non-conserved residues in black. The secondary structure is described above the sequences. Interfaces 1 and 2 are highlighted in black and red boxes respectively. Xl, *Xenopus laveis (marked green)*; Hs, *Homo sapiens*; Dm, *Drosophila melanogaster*; Sp, *S. pombe (marked red)*; Ct, *Chaetomium thermophilum*; An, *Aspergillus nidulans*; Kl, *Kluyveromyces lactis*; Ag, *Ashbya gossypii*; Kw, *Kluyveromyces waltii*; Sk, *Saccharomyces kluyveri* (marked blue), S.cas, *Shorea crassa*; Sc, *S. cerevisiae*.

Figure 3 supplement 1: yeast dimeric TOG arrays form a TOG square assembly in solution as measured by cysteine crosslinking and mass-spectrometry.

A) Mass-spectrometry based strategy for disulfide peptide mapping for Sk-Alp14 S180C L304C mutant reveals sequences of peptides in interface 1 form crosslinked disulfide confirming the conformation of interface 1 is observed in solution. Top, chemical modification strategy for differential alkylation to modify cysteines and detect disulfides.

B) LCMS/MS traces for two peptides showing the mass units identifying these peptides with cysteine modified by alkylation with a mass of 105-Da.

Figure 4 supplement 1: Inactivating interfaces 1 and 2 destabilizes the TOG square organization but does not influence αβ-tubulin binding activity.

A) Purification of INT1 mutant. Top, SEC-elution profile and trace for INT1 mutant showing it behaves homogenously similar to wt-Alp14-dimer. Bottom panel show SDS-PAGE for SEC purified fractions.

B) Purification of INT2 mutant. Top, SEC-elution profile and trace for INT2 showing it behaves homogenously similar to wt-Alp14-dimer. Bottom panel shows SDS-PAGE of SEC purified fractions.

C) Purification of INT12 mutant. Top, SEC-elution profile and trace for INT12 showing it behaves homogenously similar to wt-Alp14-dimer. Bottom panel shows SDS-PAGE of SEC purified fractions.

D) SEC traces for INT1:αβ-tubulin complexes at 100 (light pink) and 200 mM KCl (dark pink) at 2:4 molar ratio showing that inactivating TOG square assembly has little effect on αβ-tubulin binding. Note roughly half the αβ-tubulin dissociates at 200 mM KCl due to rapid exchange by TOG2. SDS-PAGE for fractions are shown **below**.

E) SEC traces for INT2:αβ-tubulin complexes at 100 (light green) and 200 mM KCl (dark green) at 2:4 molar ratio showing that inactivating TOG square assembly has little effect on αβ-tubulin binding. Note roughly half the αβ-tubulin dissociates at 200 mM KCl due to rapid exchange by TOG2. SDS-PAGE for fractions are shown **below**.

F) SEC traces for INT1:αβ-tubulin complexes at 100 (light grey) and 200 mM KCl (dark grey) at 2:4 molar ratio showing that inactivating TOG square assembly has little effect on αβ-tubulin binding. Note roughly half the αβ-

tubulin dissociates at 200 mM KCl due to rapid exchange by TOG2. SDS-PAGE for fractions are shown **below**.

Figure 5 supplement 1: Strategy to promote αβ-tubulin polymerization using DRP-ΔN and the structural comparison of DRP and DRP-ΔN interfaces with αβ-tubulin.

A) SEC –trace for the purified DRP-ΔN mutant.

B) SEC-trace of 1:2:2 TOG1-TOG2:αβ-tubulin: DRP-ΔN complex (blue) in comparison to DRP-ΔN (red) and αβ-tubulin (black).

C) and **D)** SDS-PAGE fractions shown in A and B, respectively.

E) Models of the DRP-ΔN (orange) and DRP (yellow). Comparison of their binding interfaces with αβ-tubulin dimer reveals a slightly small interface.

F) View of αβ-tubulin binding interfaces of DRP-ΔN (orange) and DRP (yellow). Note the decrease in interface surface at the fifth ankyrin repeats.

Figure 5 supplement 2: X-ray Crystallographic structure determination of 1:2:1 Sk-Alp14-monomer:αβtubulin: DRP-ΔN complex .

A) View of rectangular 1:2:1 TOG1-TOG2:αβ-tubulin:DRP-ΔN crystals formed in the same conditions as crystals in Figure S3A.

B) Top, molecular replacement solution to identify positions for αβ-tubulin in the 1:2:1 TOG1-TOG2:αβ-tubulin: DRP-ΔN unit cell. Bottom, molecular replacement solution to identify positions for TOG domains in the 1:2:1 TOG1-TOG2:αβ-tubulin: DRP-ΔN unit cell.

C) 3.3-Å resolution refined 2Fo-Fc density map with 1σ contour of the native 1:2:1 TOG1-TOG2:αβ-tubulin: DRP-ΔN assembly showing the organization of the extended assembly and the modeled protein subunits.

D) Top, Top-end view of the unit-cell packing arrangement of 1:2:1 TOG1-TOG2:αβ-tubulin: DRP-ΔN extended complexes (shown in multiple colors). Bottom, 90° rotation with extended packing leads to side view of the unit cell arrangement.

E) The TOG1-TOG2 polymerized αβ-tubulin (red) structure is highly curved compared to most known αβ-tubulin polymers, such as assemblies of stathmin/RB3 complexes (GDP in cyan and GTP in yellow) and straight MT protofilament (green). A similar analysis to that previously published (Brouhard and Rice, 2014). Data is also described in Table S5.

Figure 7 supplement 1: All-atom docking models for structures superimposed onto curved protofilament plus-ends.

A) An all-atom model for TOG square bound to four αβ-tubulin docked onto the protofilament plus-end by overlaying the terminal αβ-tubulin with the αβ-tubulin bound onto TOG1. Note some minor steric clashes between TOG2-αβ-tubulin from the second αβ-tubulin and penultimate αβ-tubulin in the protofilament (green arrows). These steric contact may induce destabilization of the TOG square at interface 1 near the site of polymerization.

B) An all-atom model for TOG square bound to four αβ-tubulin docked onto the protofilament plus-end by overlaying the terminal αβ-tubulin with the

αβ-tubulin bound onto TOG2. Note the TOG1-αβ-tubulin from the second αβ-tubulin is retracted 10-Å away from the penultimate αβ-tubulin in the protofilament (green arrows). This suggests that TOG2-αβ-tubulin docking has no effect on destabilizing the TOG square.

C) An overlay of A and B is shown.

D) Supplementary References:

Brouhard, G.J., and Rice, L.M. (2014). The contribution of alphabeta-tubulin curvature to microtubule dynamics. J Cell Biol *207*, 323-334.

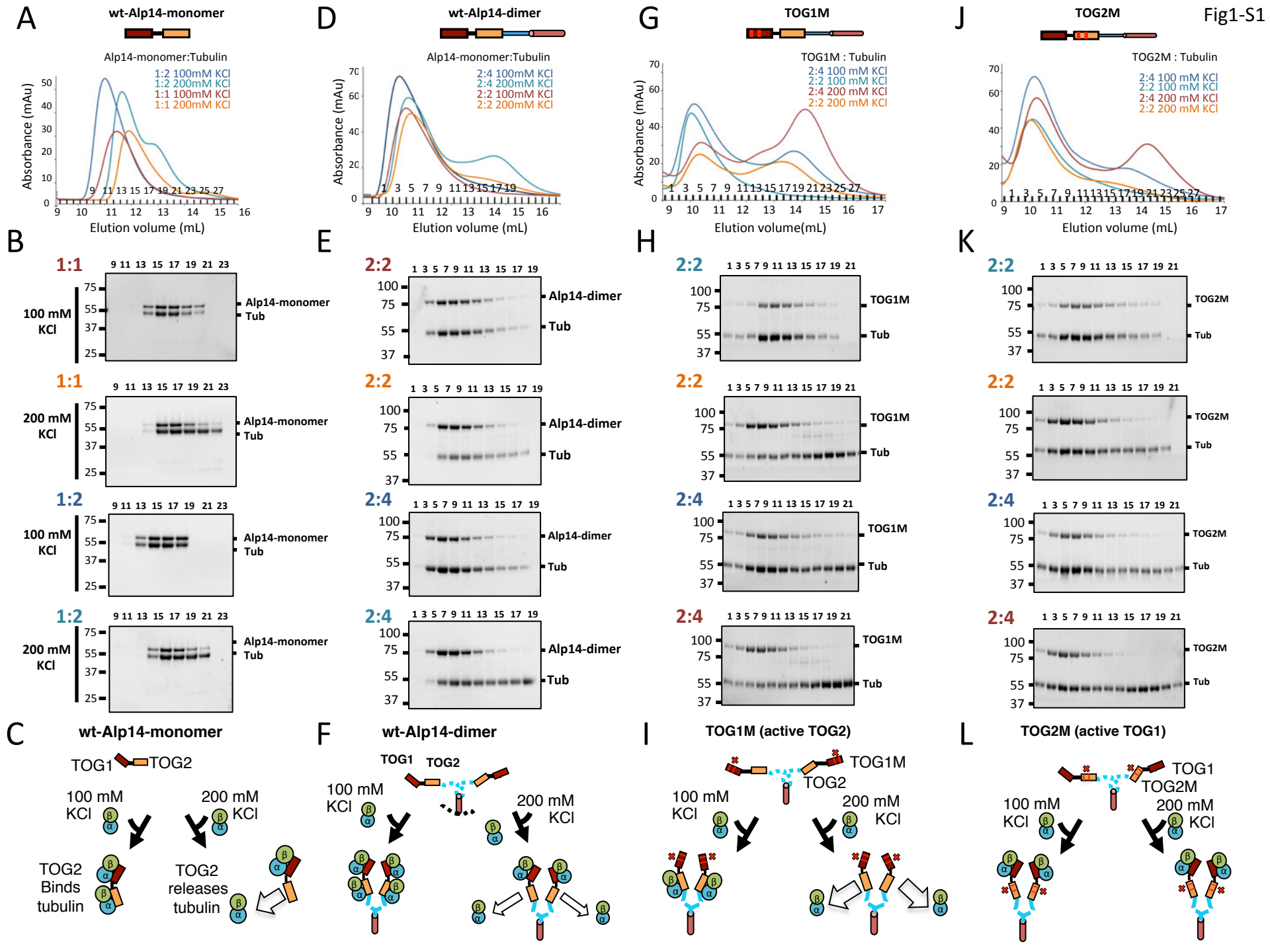
A
wt-Alp14-monomer
Alp14-monomer:Tubulin
1:2 100mM KCl
1:2 200mM KCl
1:1 100mM KCl
1:1 200mM KCl
Absorbance (mAu)
Elution volume (mL)
D
wt-Alp14-dimer
Alp14-monomer:Tubulin
2:4 100mM KCl
2:4 200mM KCl
2:2 100mM KCl
2:2 200mM KCl
Absorbance (mAu)
Elution volume (mL)
G
TOG1M
TOG1M : Tubulin
2:4 100 mM KCl
2:2 100 mM KCl
2:4 200 mM KCl
2:2 200 mM KCl
Absorbance (mAu)
Elution volume(mL)
J
TOG2M
TOG2M : Tubulin
2:4 100 mM KCl
2:2 100 mM KCl
2:4 200 mM KCl
2:2 200 mM KCl
Elution volume (mL)
Fig1-S1
B
1:1
100 mM KCl
Alp14-monomer
Tub
1:1
200 mM KCl
Alp14-monomer
Tub
1:2
100 mM KCl
Alp14-monomer
Tub
1:2
200 mM KCl
Alp14-monomer
Tub
E
2:2
Alp14-dimer
Tub
2:2
Alp14-dimer
Tub
2:4
Alp14-dimer
Tub
2:4
Alp14-dimer
Tub
H
2:2
TOG1M
Tub
2:2
TOG1M
Tub
2:4
TOG1M
Tub
2:4
TOG1M
Tub
K
2:2
TOG2M
Tub
2:2
TOG2M
Tub
2:4
TOG2M
Tub
2:4
TOG2M
Tub
C
wt-Alp14-monomer
TOG1
TOG2
100 mM KCl
200 mM KCl
TOG2 Binds tubulin
TOG2 releases tubulin
F
wt-Alp14-dimer
TOG1
TOG2
100 mM KCl
200 mM KCl
I
TOG1M (active TOG2)
TOG1M
TOG2
100 mM KCl
200 mM KCl
L
TOG2M (active TOG1)
TOG1
TOG2M
100 mM KCl
200 mM KCl

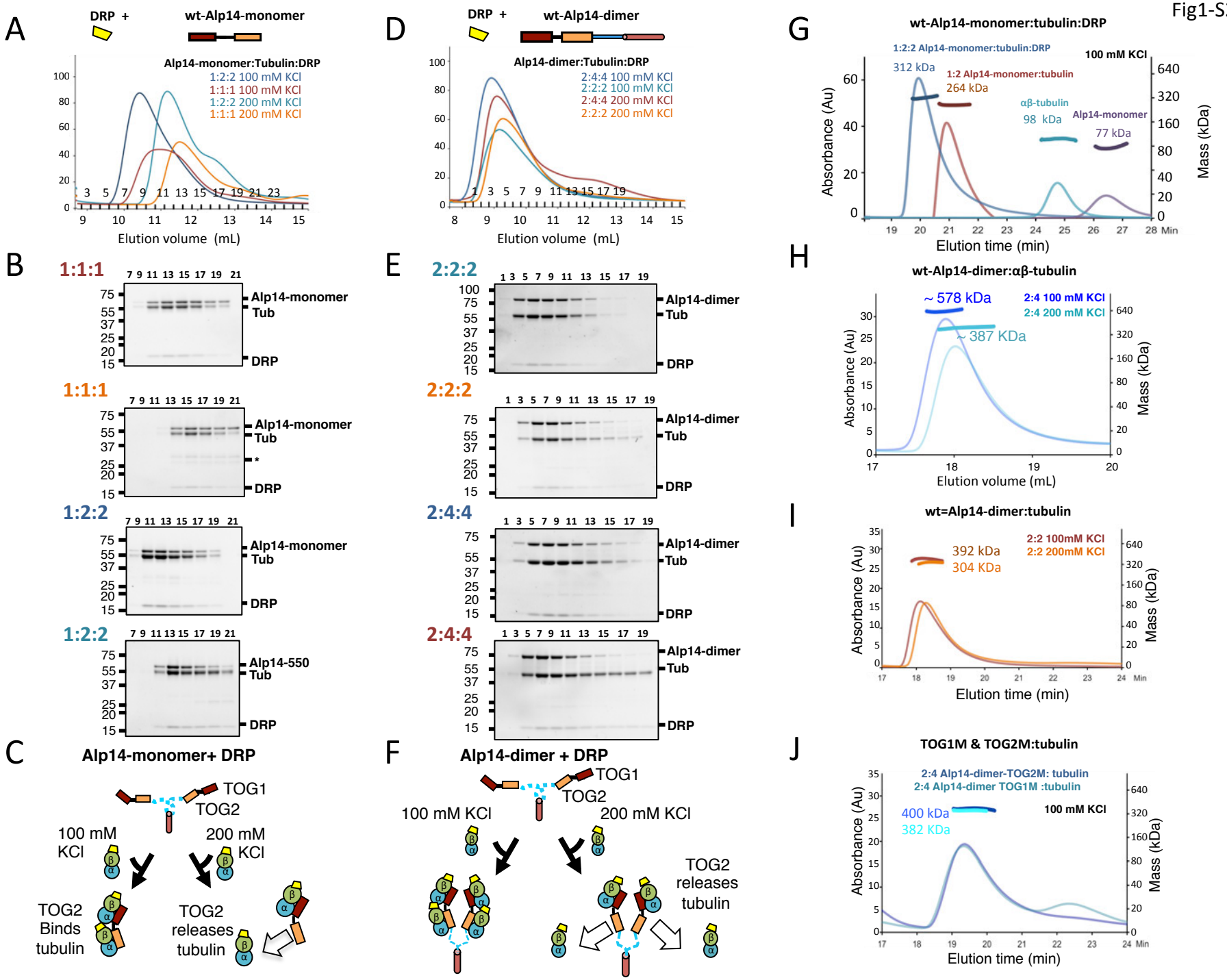
A
DRP +
wt-Alp14-monomer
Alp14-monomer:Tubulin:DRP
1:2:2 100 mM KCl
1:1:1 100 mM KCl
1:2:2 200 mM KCl
1:1:1 200 mM KCl
Elution volume (mL)
D
DRP +
wt-Alp14-dimer
Alp14-dimer:Tubulin:DRP
2:4:4 100 mM KCl
2:2:2 100 mM KCl
2:4:4 200 mM KCl
2:2:2 200 mM KCl
Elution volume (mL)
G
wt-Alp14-monomer:tubulin:DRP
1:2:2 Alp14-monomer:tubulin:DRP
100 mM KCl
312 kDa
1:2 Alp14-monomer:tubulin
264 kDa
αβ-tubulin
98 kDa
Alp14-monomer
77 kDa
Absorbance (Au)
Mass (kDa)
Elution time (min)
B
1:1:1
Alp14-monomer
Tub
DRP
1:1:1
Alp14-monomer
Tub
*
DRP
1:2:2
Alp14-monomer
Tub
DRP
1:2:2
Alp14-550
Tub
DRP
E
2:2:2
Alp14-dimer
Tub
DRP
2:2:2
Alp14-dimer
Tub
DRP
2:4:4
Alp14-dimer
Tub
DRP
2:4:4
Alp14-dimer
Tub
DRP
H
wt-Alp14-dimer:αβ-tubulin
~ 578 kDa
2:4 100 mM KCl
2:4 200 mM KCl
~ 387 KDa
Absorbance (Au)
Mass (kDa)
Elution volume (mL)
I
wt=Alp14-dimer:tubulin
392 kDa
304 kDa
2:2 100mM KCl
2:2 200mM KCl
Absorbance (Au)
Mass (kDa)
Elution time (min)
C
Alp14-monomer+ DRP
TOG1
TOG2
100 mM KCl
200 mM KCl
TOG2 Binds tubulin
TOG2 releases tubulin
F
Alp14-dimer + DRP
TOG1
TOG2
100 mM KCl
200 mM KCl
TOG2 releases tubulin
J
TOG1M & TOG2M:tubulin
2:4 Alp14-dimer-TOG2M: tubulin
2:4 Alp14-dimer TOG1M :tubulin
400 kDa
382 KDa
100 mM KCl
Absorbance (Au)
Mass (kDa)
Elution time (min)

A

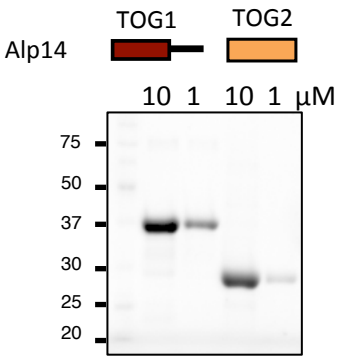

Salt(KCl)	K_d (nM)	K_d (nM)
100 mM	72.88	173.2
200 mM	1530	3250
	(~20-fold)	(~20-fold)

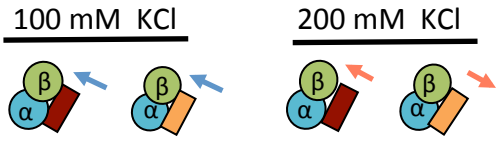

B

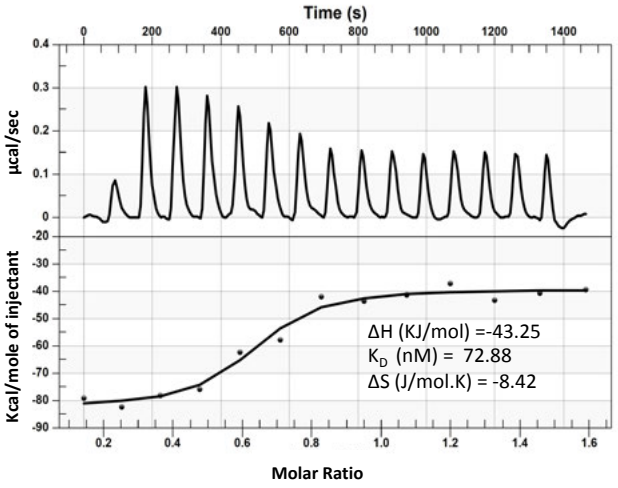

C

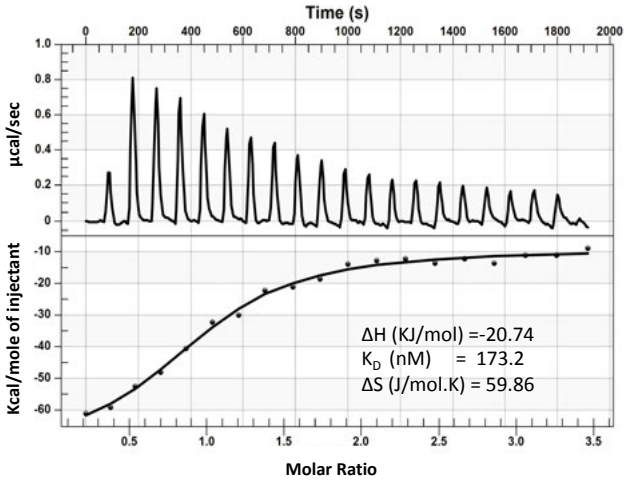

D

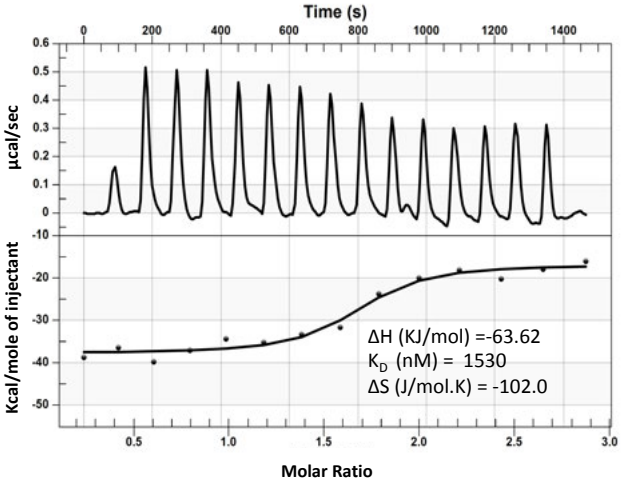

E

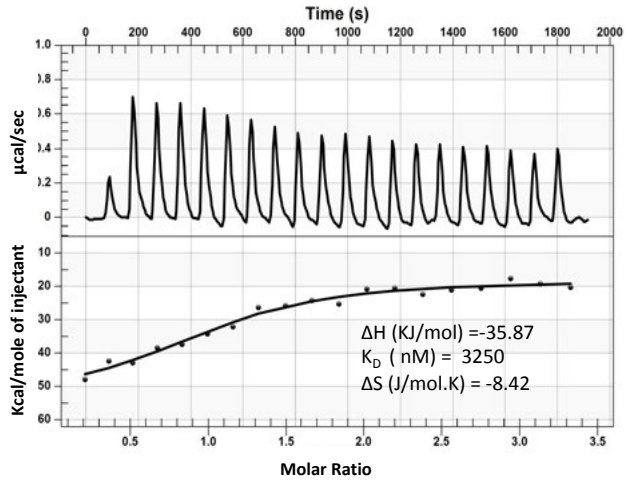

A

Sk-Alp14-monomer:αβ-tubulin:DRP crystals

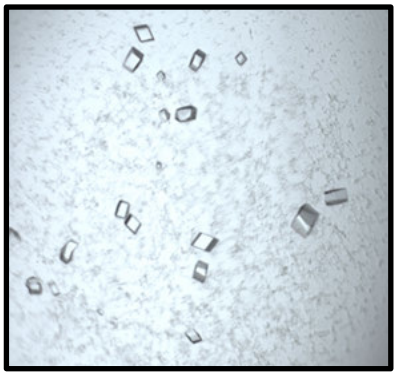

D

Map after MR (2Fo-Fc)

E

Map after DM (2Fo-Fc)

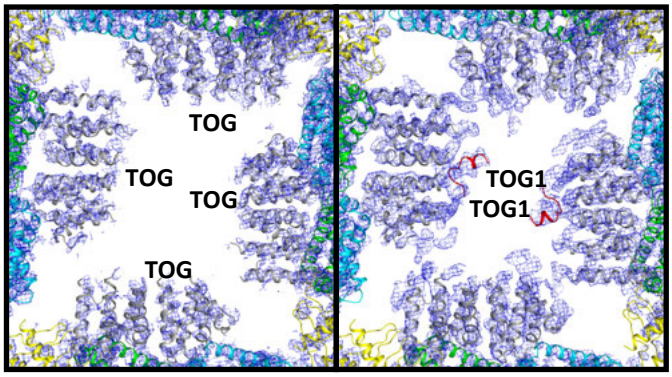

B

Molecular Replacement (MR)

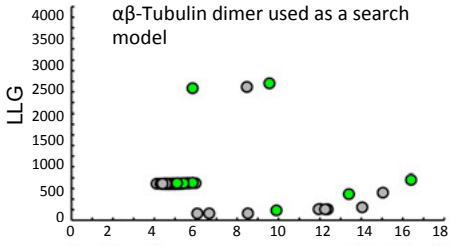

C

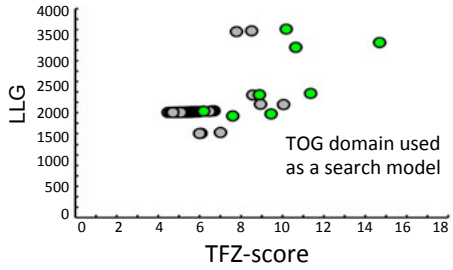

F

Sk-Alp14-monomer-SL:αβ-tubulin:DRP crystallographic unit cell

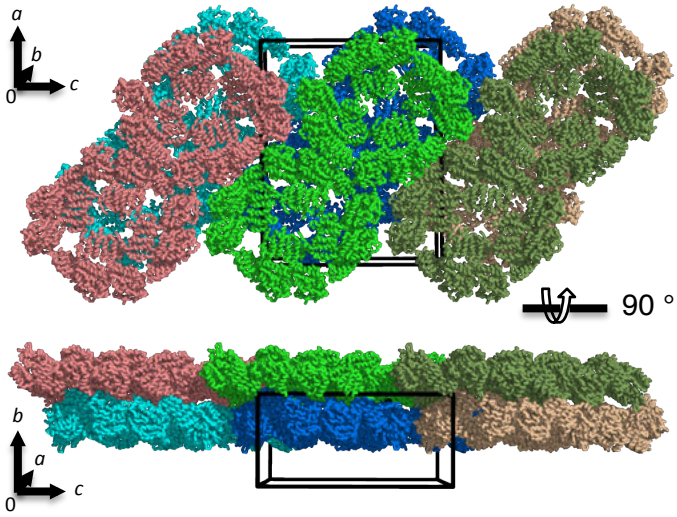

G

Sk-Alp14-monomer:tubulin:DRP map

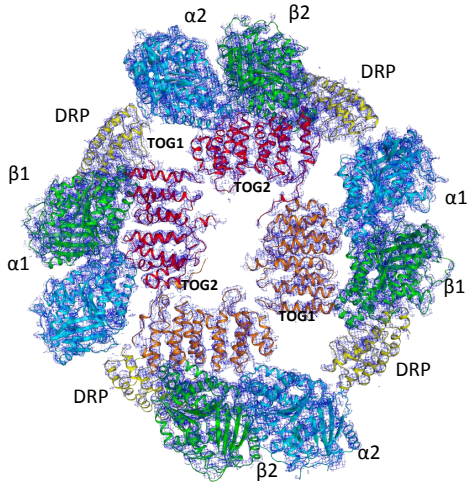

H

Sk-Alp14-monomer-SL:tubulin:DRP

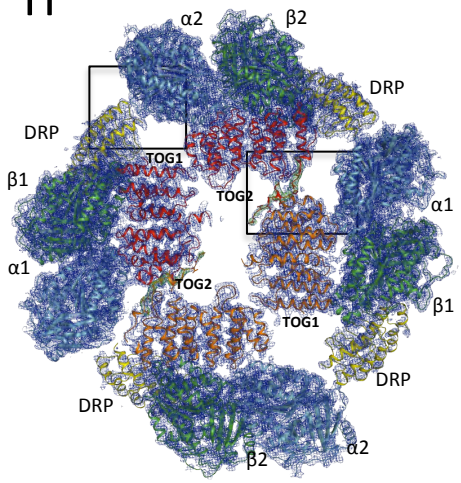

I

Close-ups in H

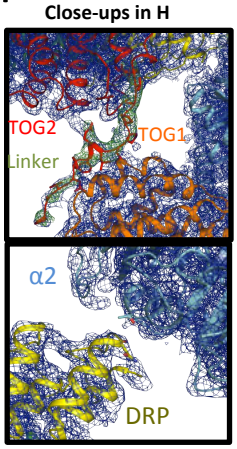

J

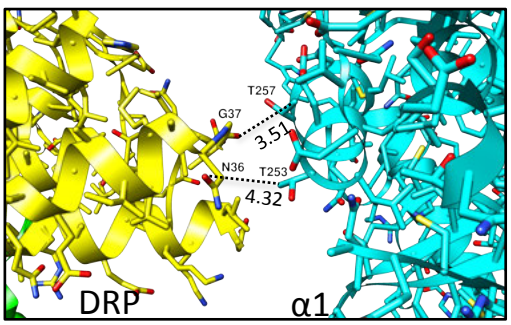

K

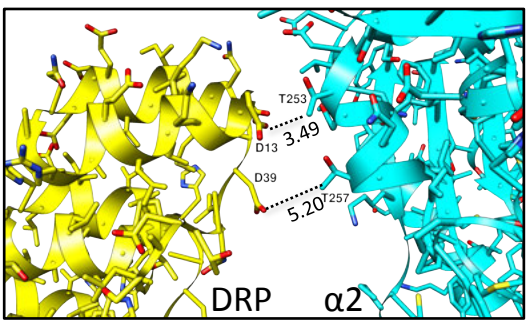

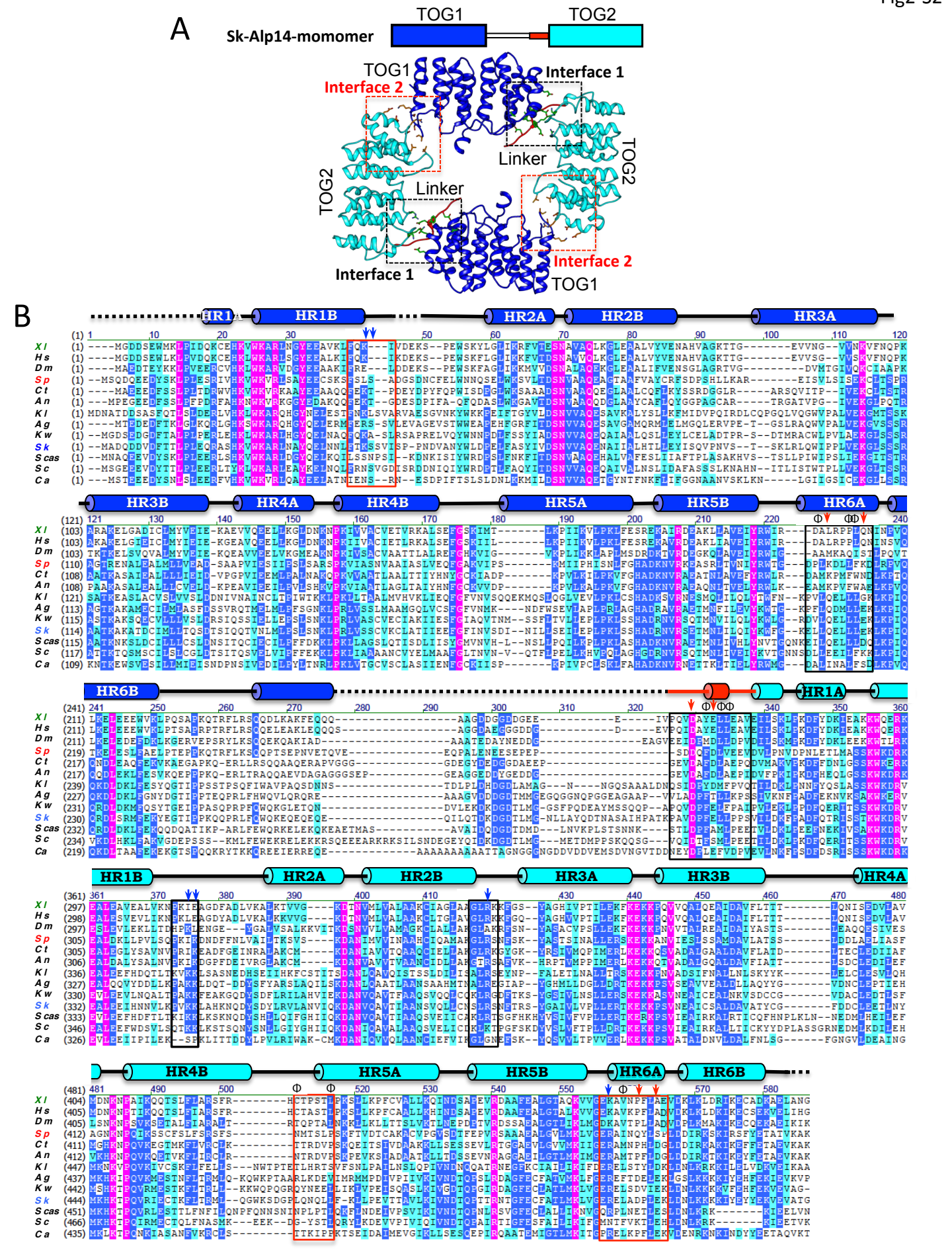
A
Sk-Alp14-momomer
TOG1
TOG2
TOG1
Interface 1
Interface 2
Linker
TOG2
Linker
TOG2
Interface 2
Interface 1
TOG1
B
HR1
HR1B
HR2A
HR2B
HR3A
HR3B
HR4A
HR4B
HR5A
HR5B
HR6A
HR6B
Xl
Hs
Dm
Sp
Ct
An
Kl
Ag
Kw
Sk
Scas
Sc
Ca

A

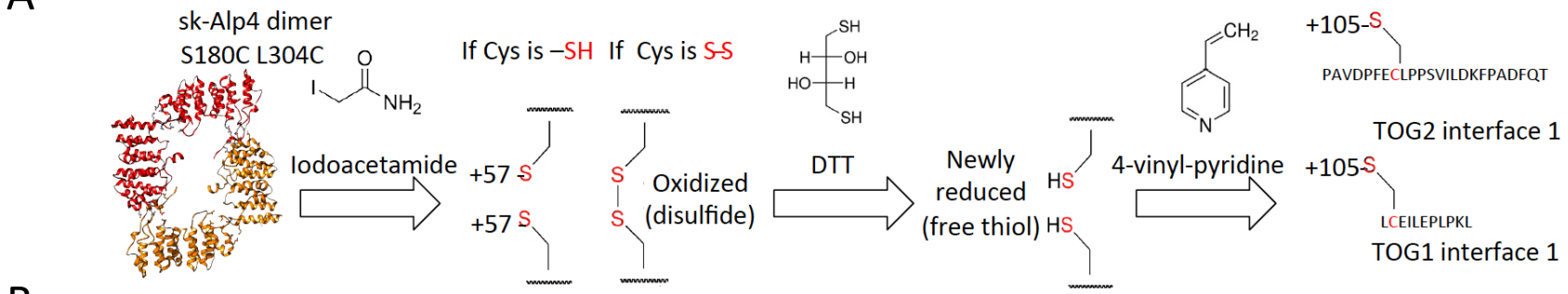
sk-Alp4 dimer
S180C L304C
Iodoacetamide
If Cys is –SH
If Cys is S-S
+57
+57
Oxidized
(disulfide)
DTT
Newly
reduced
(free thiol)
4-vinyl-pyridine
+105-S
PAVDPFECLPPSVILDKFPADFQT
TOG2 interface 1
+105-S
LCEILEPLPKL
TOG1 interface 1

B

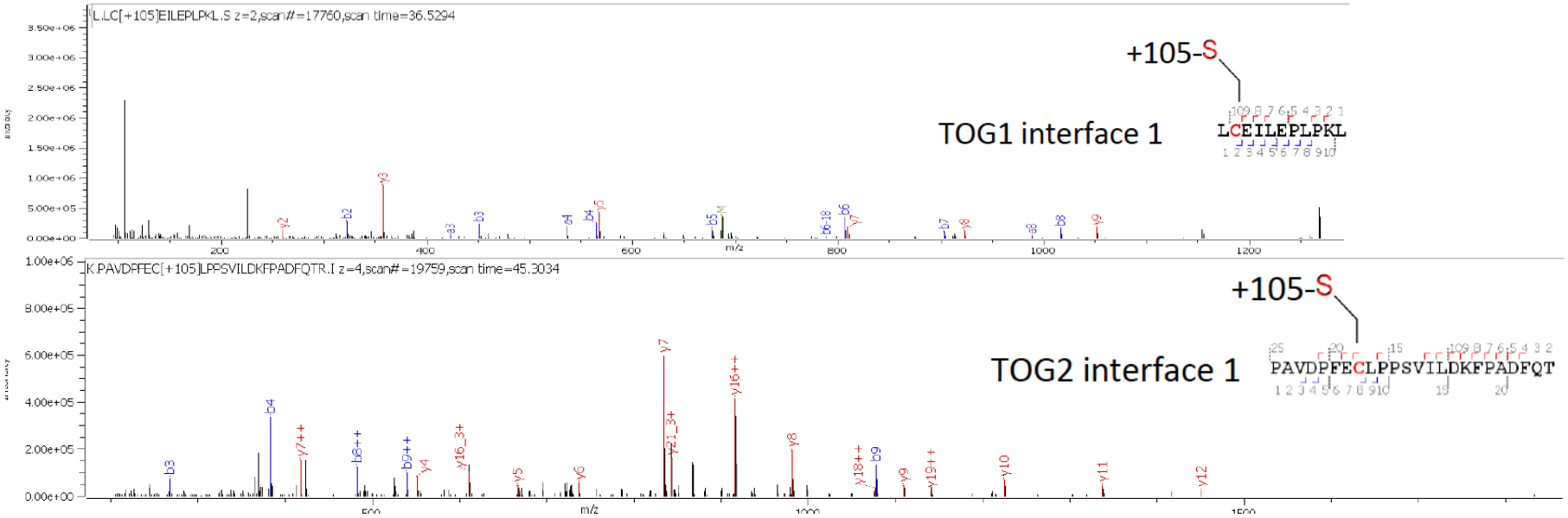
L.LC[+105]EILEPLPKL.S z=2,scan#=17760,scan time=36.5294
+105-S
TOG1 interface 1
LCEILEPLPKL
K.PAVDPFEC[+105]LPPSVILDKFPADFQTR.I z=4,scan#=19759,scan time=45.3034
+105-S
TOG2 interface 1
PAVDPFECLPPSVILDKFPADFQT
m/z

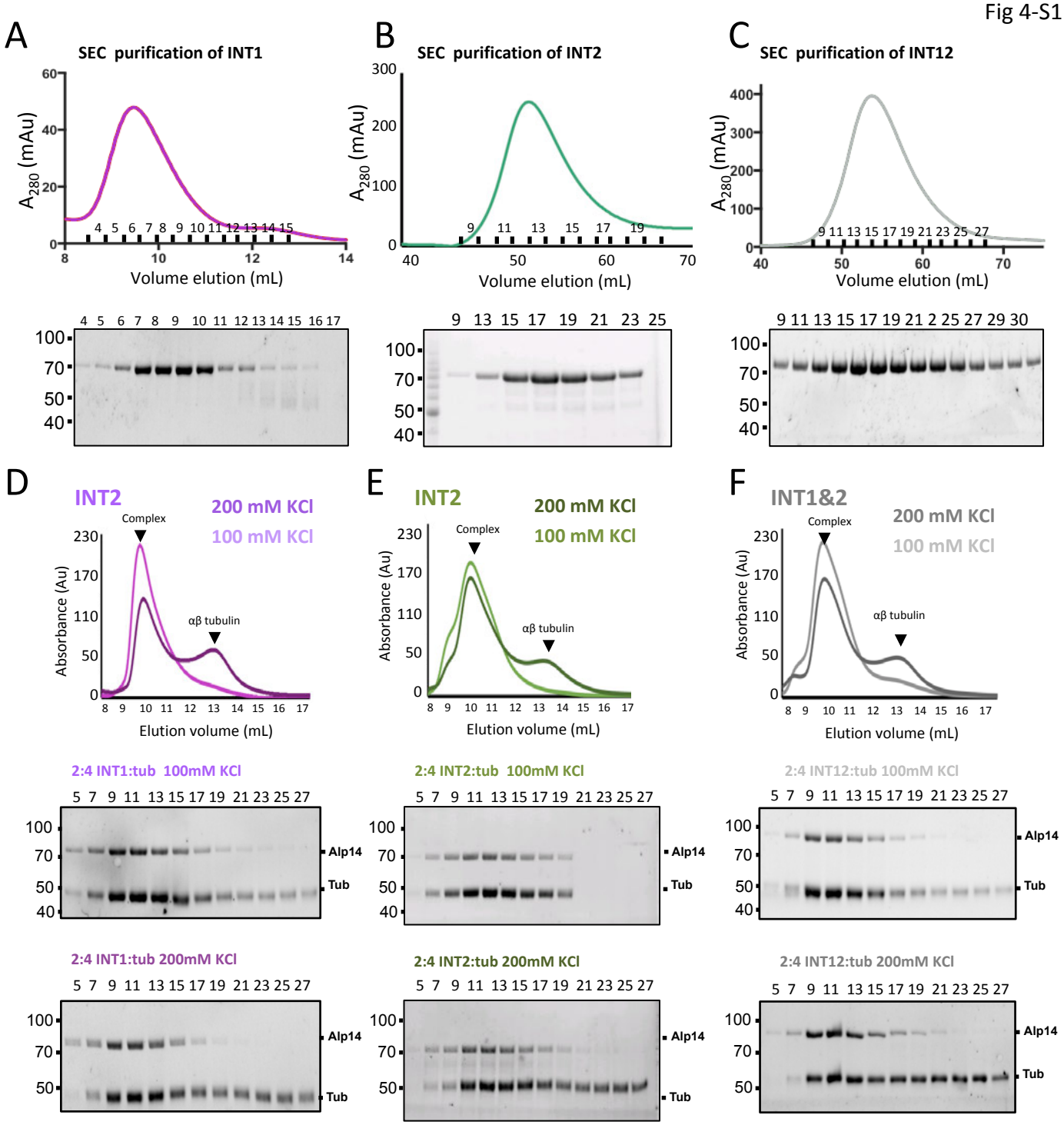
A
SEC purification of INT1
A280 (mAu)
Volume elution (mL)
B
SEC purification of INT2
A280 (mAu)
Volume elution (mL)
C
SEC purification of INT12
A280 (mAu)
Volume elution (mL)
D
INT2
200 mM KCl
100 mM KCl
Complex
αβ tubulin
Absorbance (Au)
Elution volume (mL)
E
INT2
200 mM KCl
100 mM KCl
Complex
αβ tubulin
Absorbance (Au)
Elution volume (mL)
F
INT1&2
200 mM KCl
100 mM KCl
Complex
αβ tubulin
Absorbance (Au)
Elution volume (mL)
2:4 INT1:tub 100mM KCl
2:4 INT2:tub 100mM KCl
2:4 INT12:tub 100mM KCl
2:4 INT1:tub 200mM KCl
2:4 INT2:tub 200mM KCl
2:4 INT12:tub 200mM KCl
Alp14
Tub

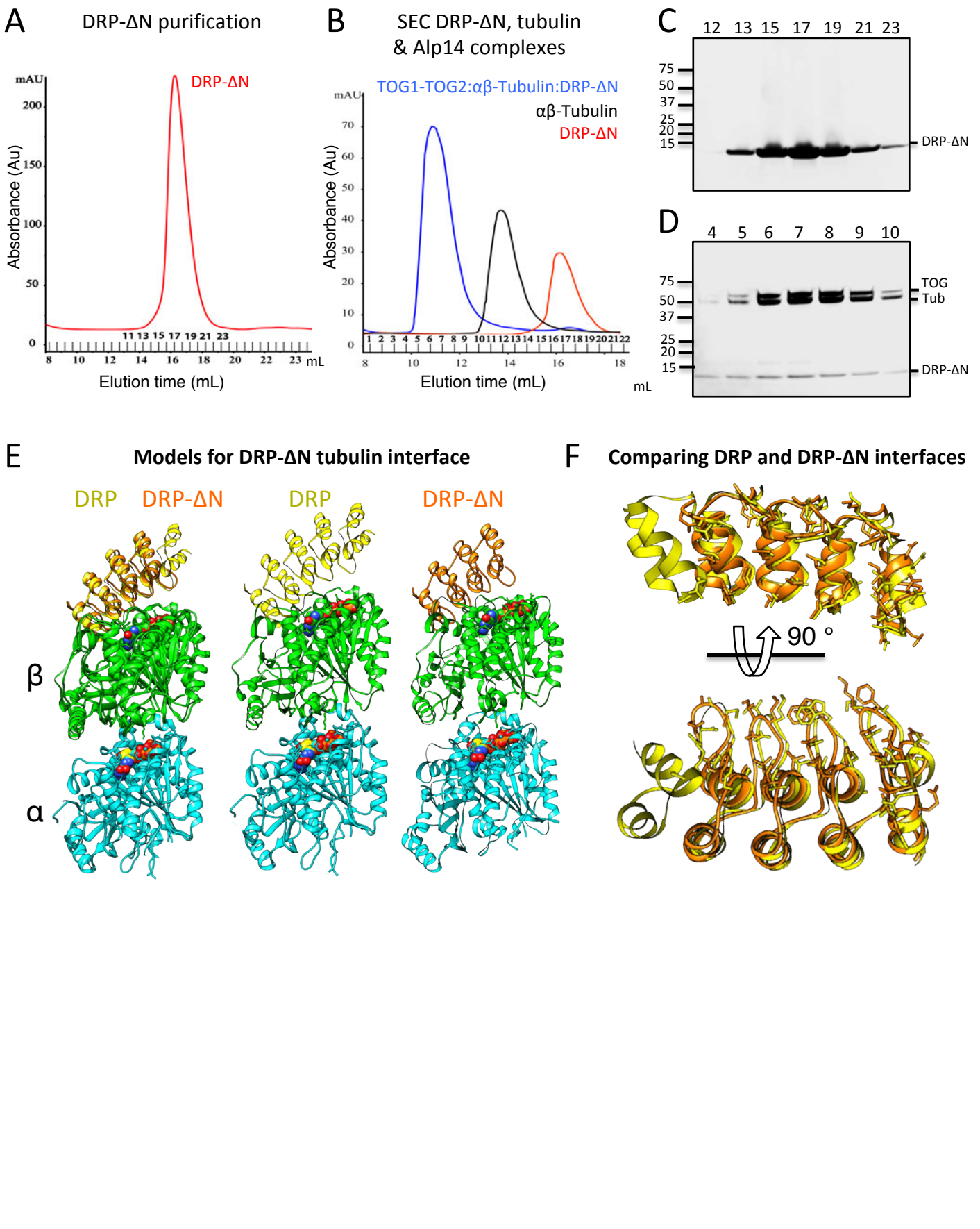
A
DRP-ΔN purification
mAU
Absorbance (Au)
DRP-ΔN
Elution time (mL)
mL
B
SEC DRP-ΔN, tubulin
& Alp14 complexes
TOG1-TOG2:αβ-Tubulin:DRP-ΔN
αβ-Tubulin
DRP-ΔN
Absorbance (Au)
Elution time (mL)
mL
C
12 13 15 17 19 21 23
75
50
37
25
20
15
DRP-ΔN
D
4 5 6 7 8 9 10
75
50
37
25
20
15
TOG
Tub
DRP-ΔN
E
Models for DRP-ΔN tubulin interface
DRP
DRP-ΔN
DRP
DRP-ΔN
β
α
F
Comparing DRP and DRP-ΔN interfaces
90 °

A **Sk-Alp14-monomer:tubulin:DRP-ΔN crystals**

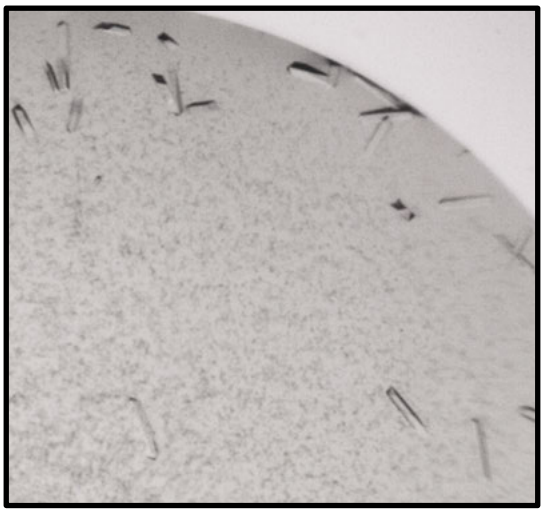

B **Molecular Replacement**

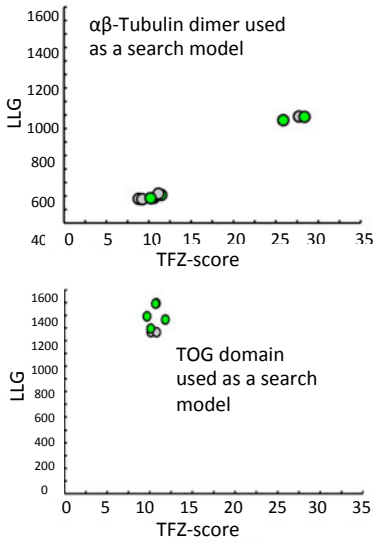

C **Map of 1:2:1-ΔN DRP**

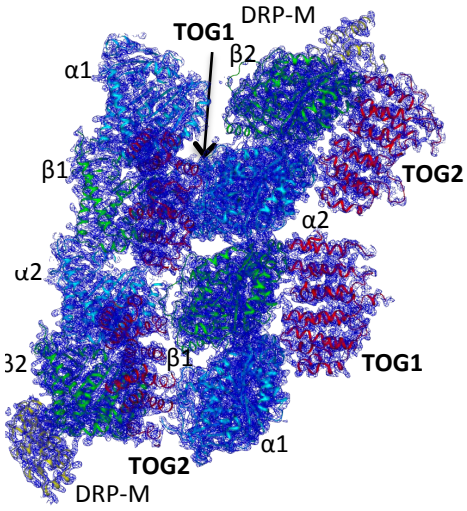

D **Packing in the crystallographic unit cell**

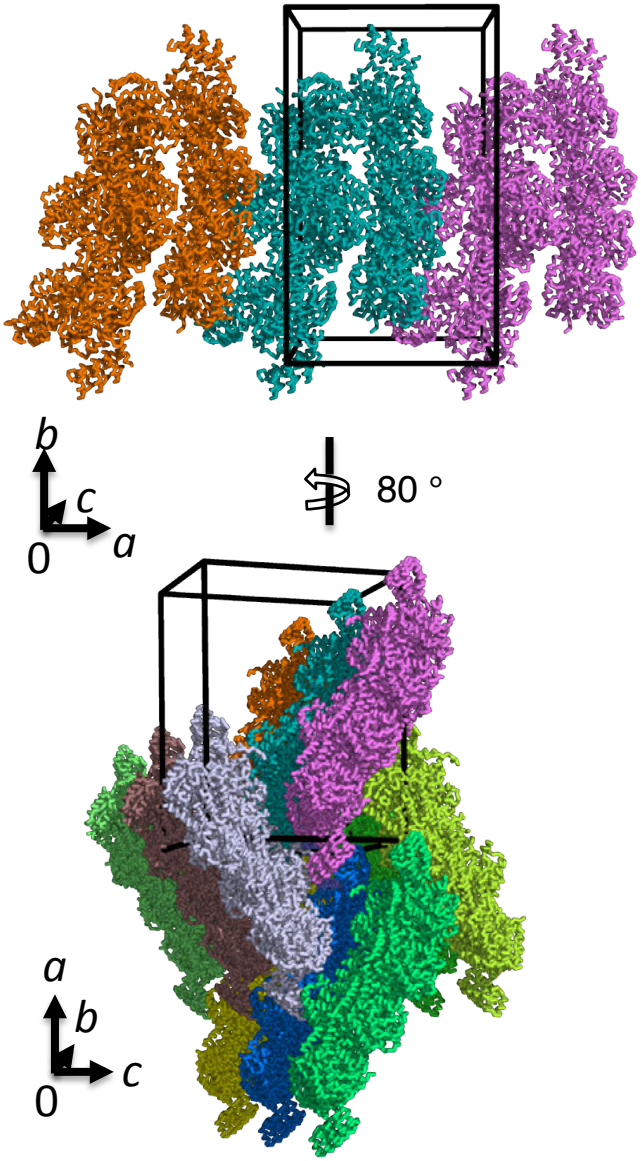

E **αβ-tubulins are highly curved in the Sk-Alp14-monomer:tubulin:DRP-ΔN structure**

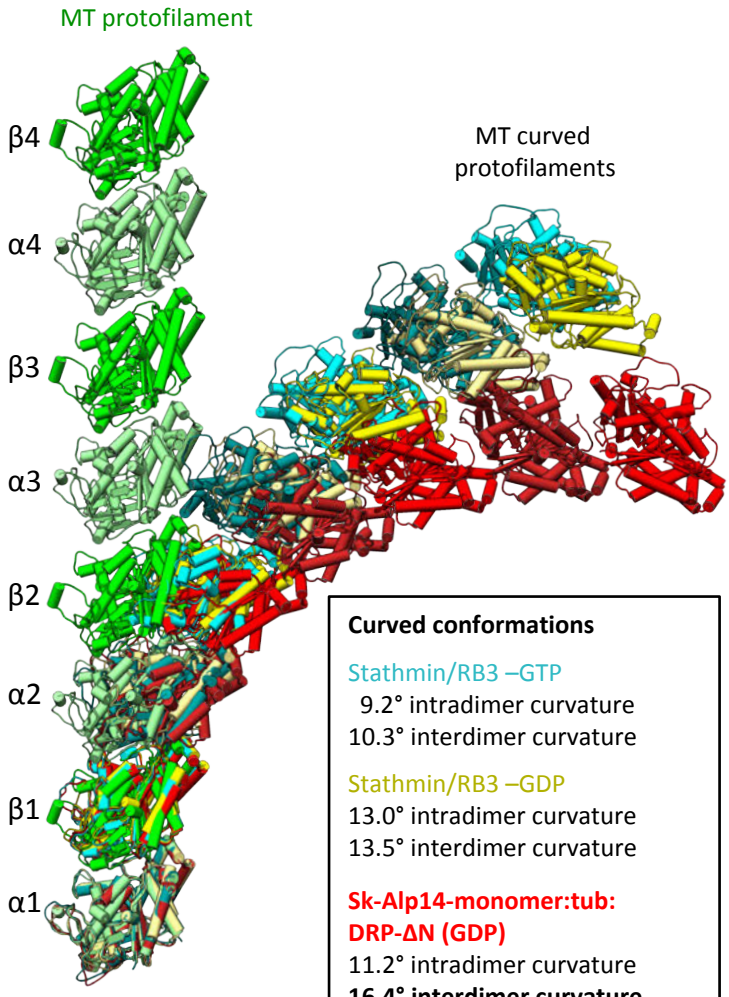

Curved conformations

Stathmin/RB3 –GTP
9.2° intradimer curvature
10.3° interdimer curvature

Stathmin/RB3 –GDP
13.0° intradimer curvature
13.5° interdimer curvature

Sk-Alp14-monomer:tub: DRP-ΔN (GDP)
11.2° intradimer curvature
16.4° interdimer curvature

A TOG1-docked

B TOG2-docked

C overlay